Environmental Science & Technology

pubs.acs.org/est

Article

Soil Emissions of Reactive Nitrogen Accelerate Summertime Surface Ozone Increases in the North China Plain

Wanshan Tan, Haolin Wang, Jiayin Su, Ruize Sun, Cheng He, Xiao Lu,* Jintai Lin, Chaoyang Xue, Haichao Wang, Yiming Liu, Lei Liu, Lin Zhang, Dianming Wu, Yujing Mu, and Shaojia Fan

Cite This: https://doi.org/10.1021/acs.est.3c01823

Read Online

ACCESS | Metrics & More | Article Recommendations | Supporting Information

ABSTRACT: Summertime surface ozone in China has been increasing since 2013 despite the policy-driven reduction in fuel combustion emissions of nitrogen oxides (NO_x). Here we examine the role of soil reactive nitrogen (N_r, including NO_x and nitrous acid (HONO)) emissions in the 2013−2019 ozone increase over the North China Plain (NCP), using GEOS-Chem chemical transport model simulations. We update soil NO_x emissions and add soil HONO emissions in GEOS-Chem based on observation-constrained parametrization schemes. The model estimates significant daily maximum 8 h average (MDA8) ozone enhancement from soil N_r emissions of 8.0 ppbv over the NCP and 5.5 ppbv over China in June−July 2019. We identify a strong competing effect between combustion and soil N_r sources on ozone production in the NCP region. We find that soil N_r emissions accelerate the 2013−2019 June-July ozone increase over the NCP by 3.0 ppbv. The increase in soil N_r ozone contribution, however, is not primarily driven by weather-induced increases in soil N_r emissions, but by the concurrent decreases in fuel combustion NO_x emissions, which enhance ozone production efficiency from soil by pushing ozone production toward a more NO_x-sensitive regime. Our results reveal an important indirect effect from fuel combustion NO_x emission reduction on ozone trends by increasing ozone production from soil N_r emissions, highlighting the necessity to consider the interaction between anthropogenic and biogenic sources in ozone mitigation in the North China Plain.

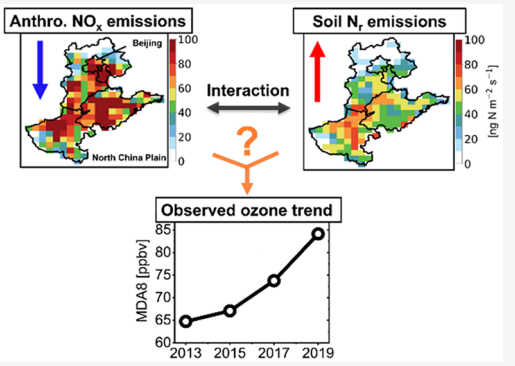

KEYWORDS: *Ozone trend, Soil emissions, Reactive nitrogen, GEOS-Chem model simulation, Interaction*

1. INTRODUCTION

Ozone near the surface is an air pollutant detrimental to human health and vegetation growth and is also a powerful atmospheric oxidant and greenhouse gas.[1−4] It is chemically produced from nitrogen oxides (NO_x = NO + NO_2), carbon monoxide (CO), and volatile organic compounds (VOCs) in the presence of sunlight. These ozone precursors are emitted from anthropogenic fuel combustion, including power plant, industry, residential, and transportation sectors and also from biogenic sources including soil and vegetation. Extensive emissions of ozone precursors have led to severe summertime ozone pollution in China, in particular the North China Plain (NCP).[5,6] Annual NO_x emissions from fuel combustion in China have been reduced by 22% from 2013 to 2019,[7,8] but the warm-season daily maximum 8 h average (MDA8) ozone over major Chinese cities has increased by 2.4 (3.3 for the NCP) ppbv $year^{-1}$ in the same period, larger than reported trends in any other region worldwide with an extensive ozone monitoring network in the same period.[9,10] These ozone increases have been attributed to decreases in aerosol loading and NO_x concentrations and changes in meteorological conditions.[9,11−15] Here, we show that enhanced ozone production from soil emissions of reactive nitrogen gases (N_r, including NO_x and nitrous acid (HONO)) with the decrease in fuel NO_x emissions serves as an important factor contributing to the increasing summertime ozone in the NCP region during 2013−2019.

Soil has been identified as an important source of N_r.[16−22] N_r emissions from soil are controlled by available soil nitrogen content and edaphic conditions such as soil water content (SWC) and temperature.[16,17,19,22,23] The NCP region occupies a large area of cultivated land (~0.3 × 10^6 km^2) that is regularly treated with intensive chemical nitrogen fertilizers and also receives extensive nitrogen deposition.[24,25] The high soil nitrogen content from both agricultural fertilizer input and deposition have led to large soil N_r emissions in the summertime.[26−29] These soil emissions are conventionally considered as biogenic sources, even though a large proportion of them are originally from anthropogenic agriculture activities.

Received: March 8, 2023
Revised: August 7, 2023
Accepted: August 9, 2023

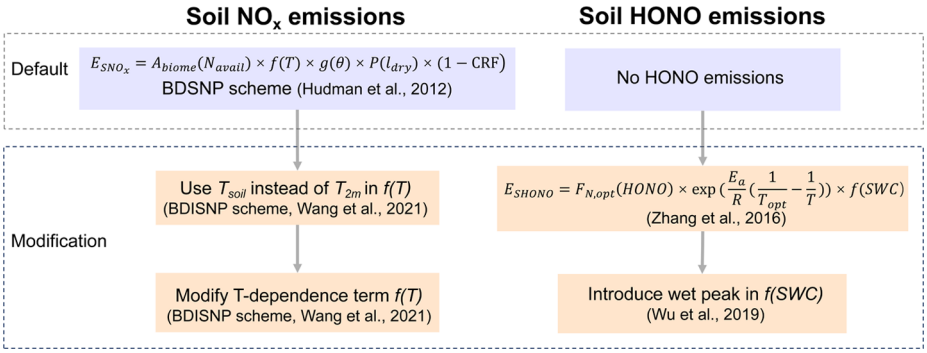

Figure 1. Improvement of soil emissions of reactive nitrogen (N_r) in the GEOS-Chem model implemented in this study. Details are described in sections 2.2 and 2.3.

A number of studies estimated significant episodic surface ozone enhancement from soil NO_x and/or HONO emissions by up to 8 ppbv.[12,22,30−33] Lu et al.[34] pointed out a competing effect between NO_x emissions from fuel combustion and soil on ozone formation in the NCP region, suggesting that soil ozone contribution may vary with changes in NO_x emissions from fuel combustion. However, the role of soil N_r ozone production in the observed increasing trends in surface ozone in China has not been recognized.

In this study, we implement and improve the estimates of soil N_r emissions over China in the chemical transport model (CTM) GEOS-Chem on the basis of published observation-constrained parametrization schemes. We validate the model estimated soil N_r emissions with reported field measurements. We then quantify the interactions between anthropogenic (from fuel combustion) and soil N_r emissions on ozone formation and, for the first time, explore the role of soil N_r emissions in the observed increasing summertime (June−July) ozone concentration in China and the NCP region during 2013−2019.

2. MATERIALS AND METHODS

2.1. GEOS-Chem Chemical Transport Model. We use GEOS-Chem version 11-02-rc (https://github.com/geoschem/geos-chem/releases/tag/v11-02-rc)[35,36] to interpret summertime ozone over China and explore the role of soil N_r emissions. The model is driven by the Modern-Era Retrospective analysis for Research and Applications, Version 2 (MERRA-2) assimilated meteorological fields.[37] We conduct nested-grid simulations over East Asia (60° to 150° E, −11° to 55° N) at 0.5°(latitude) × 0.625°(longitude) resolution, with boundary conditions archived from consistent global simulations at 2° × 2.5° resolution.

GEOS-Chem includes a state-of-the-art stratospheric and tropospheric ozone-VOCs-NO_x-aerosol-halogen chemical mechanism,[38−42] dry and wet deposition schemes for both gases and aerosols,[43−46] and a nonlocal scheme for boundary layer mixing.[47] We applied anthropogenic emissions from the latest version of the Community Emissions Data System inventory (CEDS v-2021-04-21),[48] in which the 2013−2019 anthropogenic emissions over China are adjusted to be consistent with the Multi-resolution Emission Inventory for China (MEIC) inventory.[7] Natural emissions of ozone precursors, including biogenic VOCs,[49] lightning NO_x,[50] and soil NO_x emissions,[19,34] are calculated online through the Harvard−NASA Emissions Component (HEMCO).[51] We improve the parametrization of soil NO_x emissions and add soil HONO emissions as described in Figure 1 and text below.

2.2. Modification to Soil NO_x Emission Parametrization in GEOS-Chem. The default GEOS-Chem model estimates soil NO_x emissions (E_{SNO_x}) as a function of nitrogen content and soil temperature and moisture following the Berkeley−Dalhousie Soil NO_x Parameterization (BDSNP)[19]

$$E_{SNO_x} = A_{biome}(N_{avail}) \times f(T) \times g(\theta) \times P(l_{dry}) \times (1 - \mathrm{CRF}) \quad (1)$$

where $f(T)$ is formulated as

$$f(T) = \begin{cases} 0 (T < 0\,^\circ\mathrm{C}) \\ e^{0.103T} (0\,^\circ\mathrm{C} \le T \le 30\,^\circ\mathrm{C}) \\ e^{0.103\times 30} (T > 30\,^\circ\mathrm{C}) \end{cases} \quad (2)$$

Here, N_{avail} represents available soil nitrogen mass, including nitrogen from natural pool, fertilizer input, and deposition. A_{biome} is the soil biome coefficient. $f(T)$ and $g(\theta)$ are the dependences of the soil temperature (T) and soil moisture (θ), respectively. $f(T)$ is an exponential function when the soil temperature is between 0 and 30 °C and is constant when the soil temperature exceeds 30 °C.[16] $P(l_{dry})$ represents the pulsing emission when soil is rewetted after a long dry period, and l_{dry} is the dry spell length. CRF is the canopy-reduction factor and denotes the NO_x absorption by canopy. More details are described in Hudman et al.[19] and Lu et al.[34]

We follow Wang et al.[52] to improve BDSNP to BDISNP, in which "I" stands for Iowa, by better considering T dependence. First, soil temperature in the BDSNP scheme is calculated from 2m air temperature through empirical linear relationships based on different types of soil and canopy.[16] In BDISNP, we directly obtain surface soil temperature data from the MERRA-2 data sets. We find that the June−July mean soil temperature is 1−3 °C lower than that derived from 2m air temperature for most regions and 4−6 °C lower in Tibet in 2019 (Figure S1a). Second, the BDSNP scheme indicates that soil NO_x emissions flatten at temperatures above 30 °C. However, recent field experiments over high-temperature fertilized agricultural regions have measured rapid increases in soil NO_x emissions even when temperatures increased to 40 °C.[53] Thus, in BDISNP, we modify the temperature dependence term $f(T)$ (Figure S1b) following Wang et al.[52] as

https://doi.org/10.1021/acs.est.3c01823
Environ. Sci. Technol. XXXX, XXX, XXX−XXX

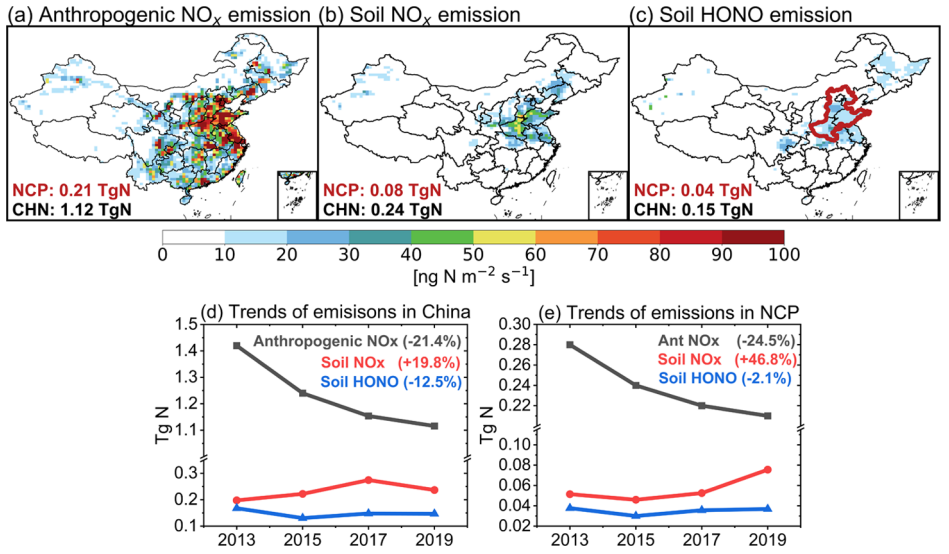

Figure 2. N_r emissions from soil and anthropogenic fossil fuel combustion in China in June−July. (a−c) Anthropogenic NO_x emissions, soil NO_x emissions, and soil HONO emissions in 2019, respectively. The total emissions for the North China Plain (NCP) and China are shown in the insets. The thick red line in (c) outlines the NCP region. (d, e) The 2013−2019 trends in emissions for China and NCP, respectively. Values in parentheses denote relative changes from 2013 to 2019.

$$f(T) = \begin{cases} 0 (T < 0\,^{\circ}\mathrm{C}) \\ e^{0.103T} (0\,^{\circ}\mathrm{C} \le T \le 20\,^{\circ}\mathrm{C}) \\ -0.009T^3 + 0.837T^2 - 22.527T + 196.149 (20\,^{\circ}\mathrm{C} < T \le 40\,^{\circ}\mathrm{C}) \\ -0.009 \times 40^3 + 0.837 \times 40^2 - 22.527 \times 40 + 196.149 (T > 40\,^{\circ}\mathrm{C}) \end{cases} \quad (3)$$

We present the June−July mean soil NO_x emissions over China in 2019 estimated from the BDISNP scheme in Figure 2b and the comparison to BDSNP scheme in Figure S2. We focus on June and July because the soil NO_x emissions in these two months are the highest across the year due to higher temperatures and frequent precipitation (Figure S3). As shown in Figure S2, the soil NO_x emissions calculated by BDISNP are 0.05 Tg N (27%) and 0.02 Tg N (45%) higher than those of the BDSNP scheme in China and the NCP region, respectively, due to the modification of $f(T)$ that reflects excessive emissions at high soil temperatures. The lower emissions in Tibet and northeastern China are due to the downward correction of soil temperature. We also compare in Figure S2c and Table S1 our estimated soil NO_x emissions with the reported field estimates over China in 2002−2017 from the literature at the corresponding time and location. We find that compared to the BDSNP scheme, the BDISNP scheme improves the correlation coefficients between observed and simulated soil NO_x emissions from 0.85 to 0.88 and slightly reduces the normalized mean bias from −67% to −61% for all observations and from −61% to −53% for the NCP region. However, there is still a substantial underestimation of soil NO_x emissions from the BDISNP scheme compared to the measurements, though this can be partly attributed to representative issues when comparing flux at 0.5° × 0.625° grids to single-point observations and uncertainties in driven meteorological fields. Improving the spatial resolution of soil NO_x emission estimate is favorable because the soil NO_x emissions have substantial heterogeneity in spatial distribution as shown in Lu et al.[34]

2.3. Implementation of Soil HONO Emissions in GEOS-Chem.

The default GEOS-Chem model includes the chemical source of HONO (e.g., from NO_x heterogeneous chemistry[54,55]) but does not consider direct HONO emissions from soil and traffic. Here we calculate hourly soil HONO emissions on each model grid based on Zhang et al.[30] and Wu et al.[56] in our GEOS-Chem simulation.

Zhang et al.[30] estimated soil HONO emissions (E_{SHONO}) from different soil types as a function of soil temperature and water content, based on laboratory experiments archived by Oswald et al.:[20]

$$E_{SHONO} = F_{N,opt}(HONO) \times \exp\left(\frac{E_a}{R}\left(\frac{1}{T_{opt}} - \frac{1}{T}\right)\right) \times f(SWC) \quad (4)$$

Here, $F_{N,opt}(HONO)$ is the optimum HONO emission flux for different soil types at a temperature of 298.15 K (T_{opt}). The soil samples used in the Oswald et al.[20] estimation were obtained from forest, pasture, grassland, wheat and cotton fields, etc., including samples from the semiarid, fertilized, and irrigated jujube field in China. In this way, the impact of fertilization on soil HONO emissions has been partly considered, even though it is simplified by using a constant $F_{N,opt}(HONO)$ derived at the specified nitrogen content of the soil at the time when the soil samples were collected. Estimation of $F_{N,opt}(HONO)$ can be improved if measurements of more soil samples are available. E_a (80 kJ mol^{-1}) is the activation energy of HONO, R (8.31 J mol^{-1} K^{-1})) is the

https://doi.org/10.1021/acs.est.3c01823
Environ. Sci. Technol. XXXX, XXX, XXX−XXX

gas constant, T and SWC are soil temperature and soil water content, respectively, and f(SWC) is the scaling function of soil water content fitted based on field measurements as will be described below.

Oswald et al.[20] showed that f(SWC) typically peaked at 0−40% soil water-holding capacity (WHC) but decreased rapidly with higher water content because of the low gas diffusion rate when soil became wet. Wu et al.[56] recently reported that soil could also release HONO at high water content (75−140% WHC) due to extracellular denitrification and anaerobic nitrate reduction under a low soil oxygen content condition, suggesting a second peak of f(SWC) at high soil water content. Wu et al.[56] provided SWC expressed as %WHC and as the ratio of water mass to soil mass, in units of %, representing the relative saturation level of soil. Here we obtained the SWC and corresponding HONO emissions measured from soil samples archived in Wu et al.[56] to fit f(SWC) as a function of SWC expressed as the ratio of water mass in soil mass (%) using Gaussian functions. The results are shown in Figure S4, which reflect both the dry and wet peaks of f(SWC).

The MERRA-2 reanalysis data set provides two parameters that consistently describe soil moisture. One is SFMC in units of m^3/m^3, representing the volume of water within the volume of bulk soil in the topmost 0−5 cm surface layer; the other is the ground wetness value GWETTOP (dimensionless), representing the relative saturation of soil for the topmost 0−5 cm. A value of 1 of GWETTOP indicates a completely saturated soil, and a value of 0 indicates a completely water-free soil. Comparisons of the MERRA-2 SFMC with the observation-constrained Soil Moisture of China by the In situ data version 1.0 (SMCI1.0) data set[57] and the ERA5 reanalysis data set show a good consistency in the magnitude and spatial patterns of soil moisture among all data sets with high spatial correlation coefficients of 0.88−0.89 (Figure S5), suggesting that the estimation of soil moisture in MERRA-2 is consistent with other independent data sets. However, SMFC differs from SWC in Wu et al.,[56] as SFMC uses the volume of water, while SWC in Wu et al.[56] uses the mass of water. Therefore, we use GWETTOP to represent SWC in units of % as an estimation of the relative saturation level of soil and test its uncertainty to the estimation of HONO emissions in the next paragraph. We then calculate the hourly gridded soil HONO emissions with the fraction of soil type of each model grid and the updated f(SWC) using eq 4, with soil temperature and moisture (GWETTOP) from the MERRA-2 data set.

Figure S6 compares our estimated soil HONO emissions over China with Wu et al.,[23] in which soil HONO emissions in 2017 were estimated by two independent bottom-up models constrained by field observations. Our estimated total soil HONO emissions in 2017 are 0.43 Tg N $year^{-1}$ over China and 0.09 Tg N $year^{-1}$ over the NCP, comparable to 0.49 and 0.08 Tg N $year^{-1}$ in Wu et al.[23] The overall spatial patterns of soil HONO emissions are also consistent, with high emissions concentrated on the Sichuan Basin (SCB), central and eastern China (including Hubei Province and the Yangtze River Delta), and the NCP region, while there are fine-scale differences in both the magnitude and spatial pattern in these emission hot spots. In contrast, using the single dry peak of f(SWC) leads to a large difference in soil HONO emissions compared to Wu et al.[23] We also show in Figure S6 and Table S2 that our estimated soil HONO emissions are generally comparable to reported field measurements (r = 0.71, NMB = −33%). The discrepancies between the simulated and measured flux reflect uncertainties in using GWETTOP to represent SWC in the parametrization, uncertainties in soil types mapping from Oswald et al.[20] and Wu et al.[56] to GEOS-Chem, the simplified consideration of fertilizer impacts, and the limited number of soil samples to estimate the relationship between soil water content and HONO emissions. We find that assuming an uncertainty of 20% in GWETTOP and its representation of SWC in units of % leads to −12−19% and 4−22% differences in the estimated HONO soil emissions in 2017 over China and NCP compared to our base estimate, respectively. More measurement studies are required to provide better observational constraints on soil HONO emission parametrization in CTMs.[21,31]

Figure 2 presents the N_r emissions from anthropogenic fuel combustion and soil emissions in June−July. We note that we do not include traffic HONO emissions due to the lack of available emission inventory, and also because the traffic HONO emissions are much smaller than those from soil and contribute negligibly to the daytime HONO except for central urban areas.[55,58,59] For June−July 2019, the anthropogenic fuel combustion NO_x emissions, soil NO_x emissions, and soil HONO emissions over China are 1.12, 0.24, and 0.15 Tg N, respectively. Specifically for the NCP region, the corresponding emissions are 0.21, 0.08, and 0.04 Tg N. We find that the soil N_r emissions account for 24% of total (soil plus fuel combustion) N_r emissions in the NCP in 2013, but this ratio substantially increases since 2013 to an exceptionally high value of 35% in 2019, with the rapid decrease in combustion sources and increase in soil NO_x emission driven by increasing soil temperature (Figure S7). We quantify the impacts of these emission trends on surface ozone formation in the next section.

2.4. Model Configuration and Evaluation of Ozone Simulation. Our BASE simulation applies the BDISNP scheme for soil NO_x emissions and implements soil HONO emissions as described above. We conducted model simulations in 2013, 2015, 2017, and 2019. For each year, we run the BASE model driven by year-specific MERRA-2 meteorology and emissions from March 1 to August 1 at the global coarse 2° × 2.5° resolution, and the boundary conditions are archived and used to drive the fine resolution simulation at 0.5° × 0.625° over East Asia from May 1 to August 1. The results for June and July are analyzed.

The configurations of the sensitivity simulations in this study are shown in Table 1. We conduct a DEFAULT simulation using the BDSNP scheme for soil NO_x emissions and no soil HONO emissions. We also conduct simulations with Chinese anthropogenic emissions and soil N_r emissions turned off separately or jointly. This study intends to quantify the ozone contribution from different sources and their interactions. To investigate the effect of anthropogenic emission changes on ozone production from soil N_r emissions, we also conduct simulations with soil N_r emissions turned on/off with the Chinese anthropogenic emissions fixed in 2013. The simulation strategy for each sensitivity experiment is the same as that for the BASE simulation except for the use of emissions and the simulation year.

We evaluate the GEOS-Chem simulation with the surface ozone observations from the Chinese National Environmental Monitoring Centre (CNEMC) network (http://www.cnemc.cn/en/), which monitors air pollutants over major cities in China since 2013 and has expanded to over 300 cities since 2015. We implement data quality control measures to exclude

https://doi.org/10.1021/acs.est.3c01823
Environ. Sci. Technol. XXXX, XXX, XXX−XXX

Table 1. Configurations of Model Simulations

model simulation ID	Chinese anthropogenic emissions of all species	soil NO_x emissions (BDISNP)	soil HONO emissions	other source[a]
BASE	√	√	√	√
DEFAULT[b]	√	√ (BDSNP)	×	√
noAnt[b]	×	√	√	√
noSNO_x[b]	√	×	√	√
noSHONO[b]	√	√	×	√
noSN_r	√	×	×	√
noAntSHONO[b]	×	√	×	√
noAntSNO_x[b]	×	×	√	√
noAntSN_r[b]	×	×	×	√
Fix_Ant2013	√ (fixed in 2013 level)	√	√	√
noSN_r_Ant2013	√ (fixed in 2013 level)	×	×	√

[a]Includes anthropogenic sources from other countries, biogenic VOCs emissions, etc. [b]Denotes that the model simulation was only performed in 2019.

unreliable hourly data following our previous study.[10,60,61] As shown in Figure 3a, the GEOS-Chem model captures the spatial distribution of observed surface MDA8 ozone in June−July well with a high spatial correlation coefficient (r) of 0.87 over all Chinese sites and reproduces the high surface ozone values in the NCP with a small bias of 0.5 ppbv. However, this small bias reflects the model overestimation of low ozone values and underestimation of high ozone values (Figure S8). The model also captures the temporal evolution of ozone for major city clusters (Figure S9). In particular, the BASE simulation with improved soil Nr emissions estimate better captures the high ozone extremes in both China and the NCP region compared to the DEFAULT simulation (Figure S8). In terms of trends, the BASE simulation produces an increase in surface ozone in the NCP region by 7.3 ppbv from 2015 to 2019, accounting for 43% of the observed ozone increases. This reflects a common difficulty for current chemical transport models to capture the large ozone increases in China for recent years,[14,55] likely due to uncertainties in the driven anthropogenic emission inventory and meteorological input, representative issues when comparing gridded model results to observations at urban sites, and model limitation in chemistry schemes.[7,12,62,63] We also compare the simulated HONO concentrations to observed values during June 2017 at Wangdu, a rural county in the central NCP. The DEFAULT model with no soil HONO emissions shows a large negative bias of −74.8% to the observed HONO concentrations averaged over the observation period. The BASE simulation significantly improves the low bias to −8.2%, though the simulation tends to overestimate daytime HONO concentrations (Figure S10).

3. RESULTS AND DISCUSSION

3.1. Ozone Contribution from Soil N_r Emissions.

Figure 3 examines the June−July mean contribution of soil NO_x, HONO, and their combined effects (soil N_r) on summertime surface ozone over China in 2019, estimated by the widely used "brute-force" method as the ozone difference between the BASE simulation and noSNO_x, noSHONO, and noSNr simulations, respectively. An example for estimating the soil N_r ozone enhancement can be expressed as

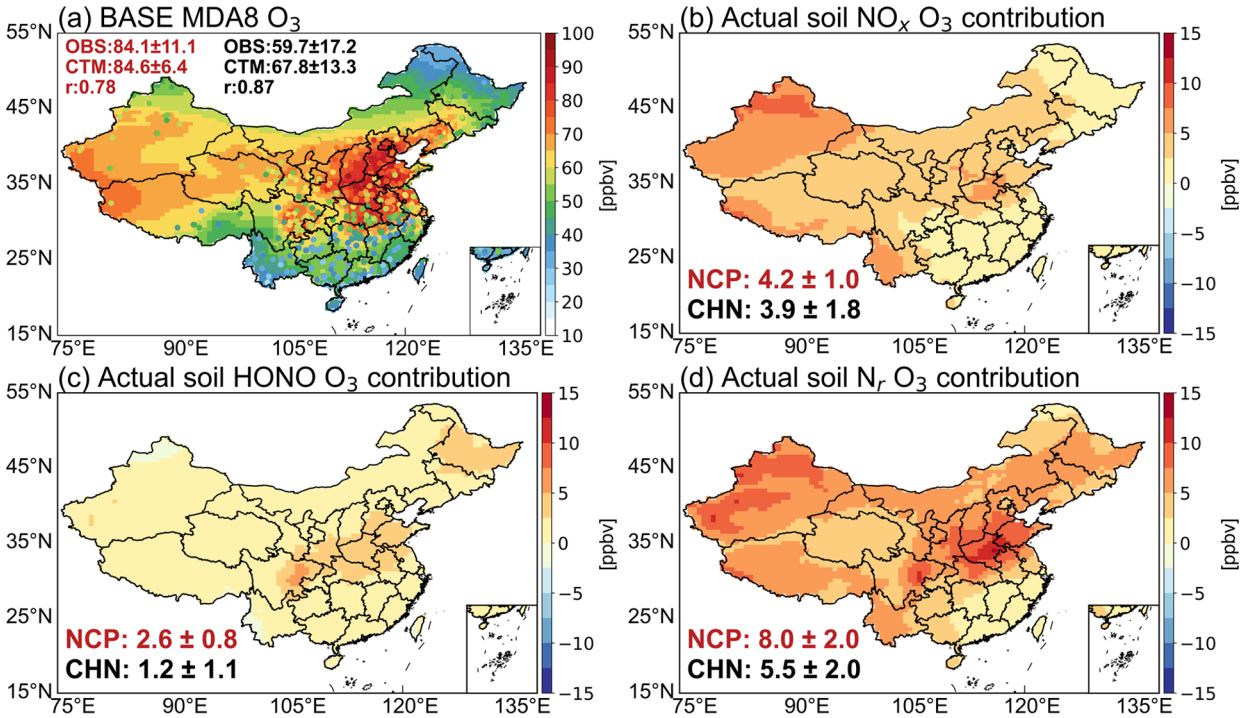

Figure 3. Surface ozone concentrations and contribution from soil N_r emissions in June-July 2019. (a) Observed (dots) and simulated (shaded) surface MDA8 ozone. Mean values ± standard deviation and the spatial correlation coefficients (r) for NCP (red) and all Chinese observation sites (black) are shown in the inset. (b−d) Actual ozone contribution from soil NO_x, HONO, and N_r (NO_x and HONO) emissions, i.e. ozone contribution from soil in the presence of other sources, respectively. Also shown are the mean values ± standard deviation averaged over the model grids.

https://doi.org/10.1021/acs.est.3c01823
Environ. Sci. Technol. XXXX, XXX, XXX−XXX

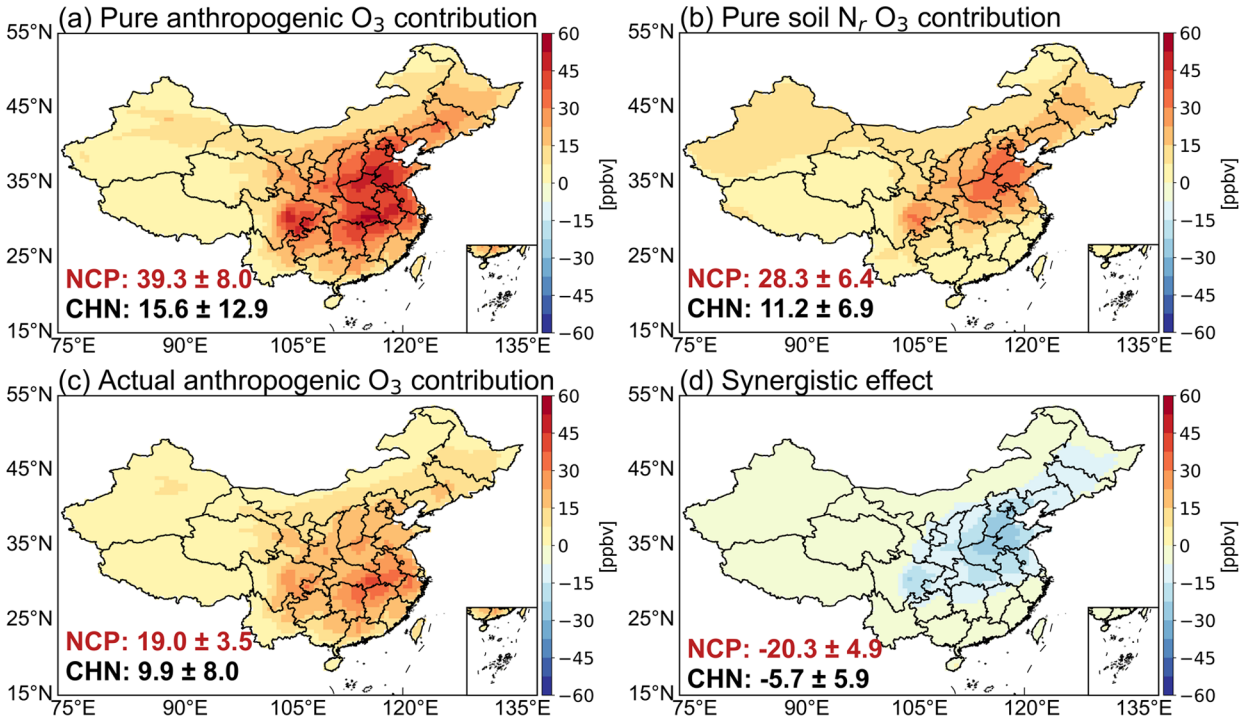

Figure 4. Actual vs pure ozone contribution from anthropogenic and soil N_r emissions to surface ozone and their interactions. (a, b) The pure ozone contribution from anthropogenic and soil N_r emissions, i.e. ozone enhancement due to anthropogenic or soil N_r emissions in the absence of the other source, respectively. (c) Actual anthropogenic emissions to ozone. (d) Synergistic effect of anthropogenic and soil N_r emissions. Also shown are the mean values ± standard deviation averaged over the model grids. See the text for the definition and derivation.

$$\text{ozone}_{\text{actualSNr}} = \text{ozone}_{\text{Base}} - \text{ozone}_{\text{noSNr}} \quad (5)$$

where the footnote of the terms on the right of the equation denotes the model simulation ID (Table 1). All values analyzed here are MDA8 ozone.

Equation 5 quantifies the actual ozone enhancement due to soil N_r emissions in the presence of anthropogenic and other sources of ozone precursors. Similarly, we can quantify the actual anthropogenic ozone enhancement by the following formula that is discussed later.

$$\text{ozone}_{\text{actualAnt}} = \text{ozone}_{\text{Base}} - \text{ozone}_{\text{noAnt}} \quad (6)$$

We find that soil NO_x emissions enhance June−July mean surface MDA8 ozone by 3.9 ppbv over China, with larger contributions of up to 9 ppbv over northwest and southwest China (Figure 3b). While soil NO_x emissions are much higher in the NCP region than those in the western part (Figure 2d), the soil NO_x ozone enhancements (4.2 ppbv) in the NCP are comparable or even smaller. This reflects the nonlinear ozone chemical production relative to NO_x levels. Surface ozone production is less sensitive to soil NO_x emissions in the NCP region due to the presence of high anthropogenic NO_x emissions,[64,65] supported by the much lower modeled surface H_2O_2 to HNO_3 values as an indicator of ozone production regime[66] in the NCP region compared to western China (Figure S11).

Soil HONO emissions produce ozone dominantly by providing both NO and OH through its photolysis (HONO → NO + OH). We estimate that they enhance June−July mean surface MDA8 ozone by 1.2 ppbv over China, 2.6 ppbv over the NCP region, and 3−7 ppbv over the SCB and Hubei Province (Figure 3c). Compared to soil NO_x emissions, ozone enhancement from soil HONO emissions is generally smaller, reflecting the smaller amounts of emissions, while the spatial patterns of ozone enhancement are more consistent with those of emissions (Figure 2c). This is because, unlike soil NO_x emissions, the hot spots of soil HONO emissions are with less intensive anthropogenic NO_x emissions and thus ozone production there is more sensitive to NO_x. In addition, OH produced from soil HONO emissions increases the atmospheric oxidation capacity and promotes ozone production (Figure S12).

Figure 3d examines the combined effect of soil NO_x and HONO emissions on surface ozone in China ($\text{ozone}_{\text{actualSNr}}$). Soil emissions of N_r led to ozone enhancement of 5.5 ppbv over China (8.1% of the total simulated MDA8 ozone) and 8.0 ppbv (9.5%) over the NCP region. We find that the soil N_r ozone enhancements are 0.4 and 1.2 ppbv larger than the additive ozone enhancement from soil NO_x and HONO emissions when averaged over China and the NCP region, respectively (Figure S13). This may reflect that HONO emissions provide extra OH radicals to promote NO_x conversion to ozone, which aggregates ozone production from additive NO_x and HONO emissions. We also find that soil N_r emissions may contribute to daily MDA8 ozone enhancement by up to 15 ppbv in episodes with high temperatures (Figure S9), suggesting their significant role in episodic ozone pollution events.

3.2. Competing Effect of Anthropogenic and Soil Emissions of N_r.

$\text{ozone}_{\text{actualSNr}}$ estimated in Figure 3d includes not only the pure contribution of soil emissions to ozone in a near-natural condition (e.g., with natural biogenic emissions but no anthropogenic emissions) but also the synergistic effect with anthropogenic emission sources.[12,67,68] Quantifying the interaction between soil and anthropogenic emissions is of particular interest because it identifies whether the presence of soil N_r emissions boosts or suppresses the contribution of

https://doi.org/10.1021/acs.est.3c01823
Environ. Sci. Technol. XXXX, XXX, XXX−XXX

ozone from existing anthropogenic emissions. Here we separately quantify ozone enhancement purely due to soil emissions and due to the synergistic effect between soil NO_x and anthropogenic emissions.

Let us assume that $ozone_{pureSNr}$ represents ozone enhancement purely due to soil N_r emissions in natural conditions and that $ozone_{pureAnt}$ represents ozone enhancement purely due to anthropogenic emissions in the presence of other natural sources but no soil N_r emissions. $ozone_{pureSNr}$ and $ozone_{pureAnt}$ can be expressed as

$$ozone_{pureSNr} = ozone_{noAnt} - ozone_{noAntSNr} \quad (7)$$

$$ozone_{pureAnt} = ozone_{noSNr} - ozone_{noAntSNr} \quad (8)$$

where $ozone_{noAntSNr}$ denotes ozone concentration in a natural condition without both soil N_r emissions and anthropogenic sources.

Ozone concentrations in the BASE simulation can then be expressed as

$$ozone_{Base} = ozone_{noAntSNr} + ozone_{pureSNr} + ozone_{pureAnt} + ozone_{synergistic} \quad (9)$$

in which $ozone_{synergistic}$ represents ozone concentrations from the synergistic interactions between the soil N_r emission and anthropogenic emissions which have not been accounted for in neither $ozone_{pureSNr}$ nor $ozone_{pureAnt}$.

We can alternatively describe ozone concentrations in the BASE simulation as

$$ozone_{Base} = ozone_{noAntSNr} + ozone_{actualSNr} + ozone_{actualAnt} - ozone_{synergistic} \quad (10)$$

in which $ozone_{synergistic}$ has been counted by twice in $ozone_{actualSNr}$ and $ozone_{actualAnt}$.

Analyses of eqs 5−10 can yield the quantitative $ozone_{synergistic}$ as

$$ozone_{synergistic} = ozone_{Base} - (ozone_{noAnt} + ozone_{noSNr}) + ozone_{noAntSNr} \quad (11)$$

Figure 4 presents the actual and pure ozone enhancement from anthropogenic and soil N_r emissions, and the synergistic effect between the two ($ozone_{synergistic}$) in 2019. We find that $ozone_{synergistic}$ is −5.7 ppbv averaged over all model grids in China and is much larger in the NCP of −20.3 ppbv and in the SCB of −15.1 ppbv. The negative values of $ozone_{synergistic}$ imply that the interactions between anthropogenic and soil N_r emissions mutually suppress ozone production from each source when the other source is included, by pushing the ozone chemical sensitivity toward a less NO_x-sensitive regime. This competing effect as a result of synergistic interactions can be further seen from the large reduction of 37% averaged over China (52% in the NCP region) from the pure anthropogenic ozone enhancement of 15.6 ppbv (39.3 ppbv) when soil N_r emissions are not considered to the actual anthropogenic ozone enhancement of 9.9 ppbv (19.0 ppbv). A similarly large reduction of 51% in China (72% in the NCP region) is found from pure soil ozone enhancement to the actual soil ozone enhancement. The larger $ozone_{synergistic}$ values in the NCP and SCB regions reflect their higher emissions from both sources. This synergistic effect to suppress ozone formation between the soil N_r and anthropogenic emissions is significantly different from that between the biogenic vegetation and anthropogenic emissions, which tends to boost ozone formation by providing extra VOCs.[67,69] The large synergistic effect also highlights the need to include soil N_r emissions for accurate attribution of the ozone source in chemical models.[34]

3.3. Contribution of Soil N_r Emissions to 2013−2019 Ozone Trends. The strong competing effect between anthropogenic and soil N_r emissions on surface ozone formation indicates that long-term trends in soil ozone enhancements are influenced not only by trends in the amount of soil N_r emission but also by concurrent changes in anthropogenic NO_x emissions. Here we examine how the ozone contribution from soil N_r emissions responds to an increase in soil N_r emissions and change in anthropogenic emissions in NCP 2013−2019 as shown in Figure 2e.

Figure 5 shows the trends in simulated surface MDA8 ozone and actual soil N_r induced ozone enhancement in June−July

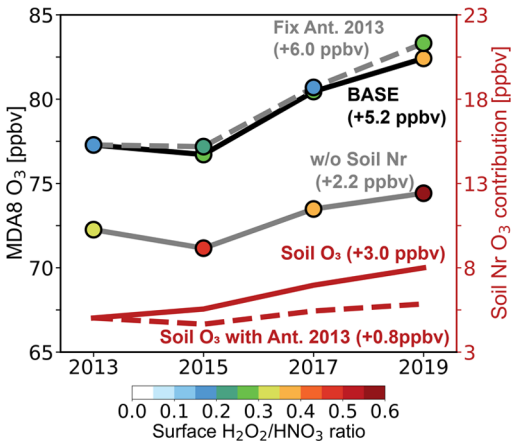

Figure 5. Soil N_r emissions accelerate ozone increases in the North China Plain. The figure shows simulated ozone trends with all sources (black solid line), trends without soil N_r emissions (gray solid line), and trends contributed by soil N_r emissions (red solid line, right *y* axis). Also shown are the simulated ozone trends with anthropogenic emissions fixed in the 2013 level (gray dashed line) and the corresponding soil N_r ozone contributions (red dashed line, right *y* axis). The colored circles denote surface H_2O_2/HNO_3 ratio in each simulation as an indicator of ozone chemical regime. The values denote ozone change in 2019 compared to 2013 level in different scenarios.

2013−2019 averaged over the NCP region. Our BASE simulation driven by year-specific meteorology and emissions shows an ozone increase of 5.2 ppbv in this period. The sensitivity simulation with soil N_r emissions excluded from the model yields an ozone increase of 2.2 ppbv, indicating that the presence of soil N_r emissions accelerates surface ozone enhancement over the NCP region by 3.0 ppbv. The difference in ozone trends between the two simulations can also be interpreted as an increase in soil N_r ozone contribution by 60% from 5.0 ppbv in 2013 to 8.0 ppbv in 2019. It highlights that the increase in ozone from soil N_r emissions is an important factor contributing to the 2013−2019 ozone trends in the NCP region that has not been recognized before.

We further examine whether the 3.0 ppbv ozone increase from soil in 2013−2019 over the NCP region is motivated by the weather-driven increase in soil emissions or by the concurrent decrease in anthropogenic emissions (mainly featured by 25% and 4% decreases in June−July NO_x and

https://doi.org/10.1021/acs.est.3c01823
Environ. Sci. Technol. XXXX, XXX, XXX−XXX

VOCs emissions). For this purpose, we conduct another sensitivity simulation (Fix_Ant2013) for 2013−2019 by fixing Chinese anthropogenic emissions in the 2013 level but with year-specific meteorology (and thus soil emissions). The results show that it reproduces a slightly larger ozone increase of 6.0 ppbv compared to 5.2 ppbv in the BASE simulation (Figure 5). The corresponding soil N_r ozone enhancement, with anthropogenic emissions fixed at the 2013 level, yields a much smaller increasing trend in 2013−2019 (0.8 ppbv higher in 2019 compared to the 2013 level), even with the same meteorology and increases in soil emissions as in the BASE simulation (Figure 5). The comparison thus clarifies that the 2013−2019 ozone increases from soil are mainly due to enhanced ozone chemical production in a more NO_x-sensitive regime with a decrease in anthropogenic NO_x emissions from fuel combustion, while weather-driven trends in soil emissions contribute little to the ozone trend when the anthropogenic NO_x level was at a relatively high value (e.g., at the 2013 level).

The above analyses reveal a significant role of soil emissions in modulating surface ozone trends via their interactions with anthropogenic emissions. This interaction can be also viewed from the perspective of the anthropogenic ozone contribution. The difference in ozone trends between the BASE and Fix_Ant2013 simulations (5.2 vs 6.0 ppbv increase from 2013 to 2019) suggests that the decrease in fuel combustion NO_x emissions since 2013 leads to a slight ozone decrease in 2013−2019 over the NCP region, but this trend largely reflects the regional compensation between the increase over the industrialized Beijing−Tianjin region and the decrease in other regions in the NCP (Figure S14). Previous studies have been focusing on the impact of changes in anthropogenic NO_x and VOCs emissions on ozone production efficiency and aerosol loading which affects ozone formation through the aerosol sink of radicals and photolysis.[11,14] Our analyses show that the 2013−2019 changes in anthropogenic emissions have also caused an indirect effect on ozone by increasing ozone production from soil N_r emissions. It further highlights the need to consider interactions between anthropogenic and biogenic soil emissions in ozone pollution mitigation.

4. IMPLICATIONS

We have estimated in this study the role of soil N_r emission in the level and trend of surface ozone in China, with a focus on the NCP region because of high soil N_r and anthropogenic emissions. We show that with an updated scheme of soil N_r emissions, our GEOS-Chem model simulation estimates significant ozone enhancement from soil emissions of reactive nitrogen by 5.5 ppbv over China and 8.0 ppbv over the NCP region averaged over June−July in 2019, both accounting for about 10% of the total ozone. We identify a strong competing effect between anthropogenic and soil N_r emissions on ozone formation over China that mutually suppresses ozone production from each source by 5.7 ppbv over China and as much as 20.3 ppbv over the NCP region. We further show that the presence of soil N_r emissions accelerates the 2013−2019 June−July surface ozone increase over the NCP region by 3.0 ppbv. The enhanced soil N_r ozone contributions are mainly driven by the concurrent decreases in NO_x emissions from fuel combustion, which enhance the ozone production efficiency from soil by pushing ozone production toward a more NO_x-sensitive regime, rather than by increases in soil N_r emissions with increasing soil temperature. However, we note that uncertainties in both anthropogenic and soil emission estimates as well as the model's inability to capture the full observed ozone trend may impact the quantitative estimate of soil ozone enhancement and their 2013−2019 trends. More direct measurements of soil N_r fluxes are crucial to better constrain soil emissions and improve the parametrization in CTMs.[70]

Our study thus reveals an important role of soil N_r emissions in modulating the surface ozone trend over China and discloses an indirect effect of anthropogenic NO_x emission reduction on ozone by increasing ozone production from soil N_r emissions. It highlights that the interaction between different ozone sources (e.g., from anthropogenic vs biogenic soil) should be considered in ozone mitigation policy design. As sharper NO_x reduction from fuel combustion is still being implemented in China, ozone contribution from soil N_r emissions may become even greater and be more sensitive to a future warming climate. Coordinated control of VOCs emissions and/or management of soil N_r emissions by improving the efficiency of nitrogen fertilizer application[34] may be effective to reduce ozone production from soil emissions.

■ ASSOCIATED CONTENT

Supporting Information

The Supporting Information is available free of charge at https://pubs.acs.org/doi/10.1021/acs.est.3c01823.

Detailed comparison of soil emissions in this study with those in the literature, supporting materials and results for parametrization of soil emissions, model evaluation of soil emissions and ozone concentrations, and simulated spatial pattern of chemical components (PDF)

■ AUTHOR INFORMATION

Corresponding Author

Xiao Lu − *School of Atmospheric Sciences, Sun Yat-sen University, and Southern Marine Science and Engineering Guangdong Laboratory (Zhuhai), Zhuhai, Guangdong 519082, People's Republic of China; Guangdong Provincial Observation and Research Station for Climate Environment and Air Quality Change in the Pearl River Estuary, Zhuhai, Guangdong 519082, People's Republic of China; Key Laboratory of Tropical Atmosphere-Ocean System, Ministry of Education, Zhuhai, China, Zhuhai, Guangdong 519082, People's Republic of China;* orcid.org/0000-0002-5989-0912; Email: luxiao25@mail.sysu.edu.cn

Authors

Wanshan Tan − *School of Atmospheric Sciences, Sun Yat-sen University, and Southern Marine Science and Engineering Guangdong Laboratory (Zhuhai), Zhuhai, Guangdong 519082, People's Republic of China; Guangdong Provincial Observation and Research Station for Climate Environment and Air Quality Change in the Pearl River Estuary, Zhuhai, Guangdong 519082, People's Republic of China; Key Laboratory of Tropical Atmosphere-Ocean System, Ministry of Education, Zhuhai, China, Zhuhai, Guangdong 519082, People's Republic of China*

Haolin Wang − *School of Atmospheric Sciences, Sun Yat-sen University, and Southern Marine Science and Engineering Guangdong Laboratory (Zhuhai), Zhuhai, Guangdong 519082, People's Republic of China; Guangdong Provincial*

https://doi.org/10.1021/acs.est.3c01823
Environ. Sci. Technol. XXXX, XXX, XXX−XXX

Observation and Research Station for Climate Environment and Air Quality Change in the Pearl River Estuary, Zhuhai, Guangdong 519082, People's Republic of China; Key Laboratory of Tropical Atmosphere-Ocean System, Ministry of Education, Zhuhai, China, Zhuhai, Guangdong 519082, People's Republic of China

Jiayin Su − *School of Atmospheric Sciences, Sun Yat-sen University, and Southern Marine Science and Engineering Guangdong Laboratory (Zhuhai), Zhuhai, Guangdong 519082, People's Republic of China; Guangdong Provincial Observation and Research Station for Climate Environment and Air Quality Change in the Pearl River Estuary, Zhuhai, Guangdong 519082, People's Republic of China; Key Laboratory of Tropical Atmosphere-Ocean System, Ministry of Education, Zhuhai, China, Zhuhai, Guangdong 519082, People's Republic of China*

Ruize Sun − *School of Atmospheric Sciences, Sun Yat-sen University, and Southern Marine Science and Engineering Guangdong Laboratory (Zhuhai), Zhuhai, Guangdong 519082, People's Republic of China; Guangdong Provincial Observation and Research Station for Climate Environment and Air Quality Change in the Pearl River Estuary, Zhuhai, Guangdong 519082, People's Republic of China; Key Laboratory of Tropical Atmosphere-Ocean System, Ministry of Education, Zhuhai, China, Zhuhai, Guangdong 519082, People's Republic of China*

Cheng He − *School of Atmospheric Sciences, Sun Yat-sen University, and Southern Marine Science and Engineering Guangdong Laboratory (Zhuhai), Zhuhai, Guangdong 519082, People's Republic of China; Guangdong Provincial Observation and Research Station for Climate Environment and Air Quality Change in the Pearl River Estuary, Zhuhai, Guangdong 519082, People's Republic of China; Key Laboratory of Tropical Atmosphere-Ocean System, Ministry of Education, Zhuhai, China, Zhuhai, Guangdong 519082, People's Republic of China*

Jintai Lin − *Laboratory for Climate and Ocean-Atmosphere Studies, Department of Atmospheric and Oceanic Sciences, School of Physics, Peking University, Beijing 100871, People's Republic of China;* orcid.org/0000-0002-2362-2940

Chaoyang Xue − *Research Center for Eco-Environmental Sciences, Chinese Academy of Sciences, Beijing 100085, China; Laboratoire de Physique et Chimie de l'Environnement et de l'Espace (LPC2E), CNRS-Université Orléans-CNES, CEDEX 2 Orléans 45071, France;* Present Address: Max Planck Institute for Chemistry, 55128 Mainz, Germany; orcid.org/0000-0001-6673-7716

Haichao Wang − *School of Atmospheric Sciences, Sun Yat-sen University, and Southern Marine Science and Engineering Guangdong Laboratory (Zhuhai), Zhuhai, Guangdong 519082, People's Republic of China; Guangdong Provincial Observation and Research Station for Climate Environment and Air Quality Change in the Pearl River Estuary, Zhuhai, Guangdong 519082, People's Republic of China; Key Laboratory of Tropical Atmosphere-Ocean System, Ministry of Education, Zhuhai, China, Zhuhai, Guangdong 519082, People's Republic of China;* orcid.org/0000-0001-6161-1874

Yiming Liu − *School of Atmospheric Sciences, Sun Yat-sen University, and Southern Marine Science and Engineering Guangdong Laboratory (Zhuhai), Zhuhai, Guangdong 519082, People's Republic of China; Guangdong Provincial Observation and Research Station for Climate Environment and Air Quality Change in the Pearl River Estuary, Zhuhai, Guangdong 519082, People's Republic of China; Key Laboratory of Tropical Atmosphere-Ocean System, Ministry of Education, Zhuhai, China, Zhuhai, Guangdong 519082, People's Republic of China*

Lei Liu − *College of Earth and Environmental Sciences, Lanzhou University, Lanzhou 730000, People's Republic of China;* orcid.org/0000-0003-2889-8900

Lin Zhang − *Laboratory for Climate and Ocean-Atmosphere Studies, Department of Atmospheric and Oceanic Sciences, School of Physics, Peking University, Beijing 100871, People's Republic of China;* orcid.org/0000-0003-2383-8431

Dianming Wu − *Key Laboratory of Geographic Information Science (Ministry of Education), School of Geographic Sciences, East China Normal University, Shanghai 200241, People's Republic of China; Institute of Eco-Chongming (IEC), Shanghai 202162, People's Republic of China;* orcid.org/0000-0002-0414-9430

Yujing Mu − *Research Center for Eco-Environmental Sciences, Chinese Academy of Sciences, Beijing 100085, China; University of Chinese Academy of Sciences, Beijing 100049, People's Republic of China;* orcid.org/0000-0002-7048-2856

Shaojia Fan − *School of Atmospheric Sciences, Sun Yat-sen University, and Southern Marine Science and Engineering Guangdong Laboratory (Zhuhai), Zhuhai, Guangdong 519082, People's Republic of China; Guangdong Provincial Observation and Research Station for Climate Environment and Air Quality Change in the Pearl River Estuary, Zhuhai, Guangdong 519082, People's Republic of China; Key Laboratory of Tropical Atmosphere-Ocean System, Ministry of Education, Zhuhai, China, Zhuhai, Guangdong 519082, People's Republic of China*

Complete contact information is available at: https://pubs.acs.org/10.1021/acs.est.3c01823

Author Contributions

X.L. designed the study. W.T. performed the model simulations and data analyses with input from H.L.W., J.S., R.S., and C.H. C.X. and Y.M. provided observations of HONO concentrations. D.W. provided estimates of soil HONO emissions. J.L., C.X., H.C.W., Y.L., L.L., L.Z., D.W., Y.M., and S.F. helped in the interpretation of results. W.T. and X.L. prepared the manuscript. All authors provided valuable comments on the manuscript.

Notes

The authors declare no competing financial interest.

■ ACKNOWLEDGMENTS

This research has been supported by the National Natural Science Foundation of China (NSFC; grant no. 42105103), the Guangdong Major Project of Basic and Applied Basic Research (grant no. 2020B0301030004), the Key-Area Research and Development Program of Guangdong Province (grant no. 2020B1111360003), and the Guangdong Science and Technology Plan Project (grant no. 2019B121201002).

■ REFERENCES

(1) Monks, P. S.; Archibald, A. T.; Colette, A.; Cooper, O.; Coyle, M.; Derwent, R.; Fowler, D.; Granier, C.; Law, K. S.; Mills, G. E.; Stevenson, D. S.; Tarasova, O.; Thouret, V.; von Schneidemesser, E.; Sommariva, R.; Wild, O.; Williams, M. L. Tropospheric ozone and its

https://doi.org/10.1021/acs.est.3c01823
Environ. Sci. Technol. XXXX, XXX, XXX−XXX

precursors from the urban to the global scale from air quality to short-lived climate forcer. *Atmospheric Chemistry and Physics* **2015**, *15* (15), 8889−8973.
(2) Turner, M. C.; Jerrett, M.; Pope, C. A., 3rd; Krewski, D.; Gapstur, S. M.; Diver, W. R.; Beckerman, B. S.; Marshall, J. D.; Su, J.; Crouse, D. L.; Burnett, R. T. Long-Term Ozone Exposure and Mortality in a Large Prospective Study. *Am. J. Respir Crit Care Med.* **2016**, *193* (10), 1134−42.
(3) Fleming, Z. L.; Doherty, R. M.; von Schneidemesser, E.; Malley, C. S.; Cooper, O. R.; Pinto, J. P.; Colette, A.; Xu, X.; Simpson, D.; Schultz, M. G.; Lefohn, A. S.; Hamad, S.; Moolla, R.; Solberg, S.; Feng, Z. Tropospheric Ozone Assessment Report: Present-day ozone distribution and trends relevant to human health. *Elementa: Science of the Anthropocene* **2018**, *6*, 12.
(4) Li, D.; Shindell, D.; Ding, D.; Lu, X.; Zhang, L.; Zhang, Y. Surface ozone impacts on major crop production in China from 2010 to 2017. *Atmospheric Chemistry and Physics* **2022**, *22* (4), 2625−2638.
(5) Wang, T.; Xue, L.; Brimblecombe, P.; Lam, Y. F.; Li, L.; Zhang, L. Ozone pollution in China: A review of concentrations, meteorological influences, chemical precursors, and effects. *Science of The Total Environment* **2017**, *575*, 1582−1596.
(6) Lu, X.; Hong, J.; Zhang, L.; Cooper, O. R.; Schultz, M. G.; Xu, X.; Wang, T.; Gao, M.; Zhao, Y.; Zhang, Y. Severe Surface Ozone Pollution in China: A Global Perspective. *Environmental Science & Technology Letters* **2018**, *5* (8), 487−494.
(7) Zheng, B.; Tong, D.; Li, M.; Liu, F.; Hong, C.; Geng, G.; Li, H.; Li, X.; Peng, L.; Qi, J.; Yan, L.; Zhang, Y.; Zhao, H.; Zheng, Y.; He, K.; Zhang, Q. Trends in China's anthropogenic emissions since 2010 as the consequence of clean air actions. *Atmospheric Chemistry and Physics* **2018**, *18* (19), 14095−14111.
(8) Zhang, Q.; Zheng, Y.; Tong, D.; Shao, M.; Wang, S.; Zhang, Y.; Xu, X.; Wang, J.; He, H.; Liu, W.; Ding, Y.; Lei, Y.; Li, J.; Wang, Z.; Zhang, X.; Wang, Y.; Cheng, J.; Liu, Y.; Shi, Q.; Yan, L.; Geng, G.; Hong, C.; Li, M.; Liu, F.; Zheng, B.; Cao, J.; Ding, A.; Gao, J.; Fu, Q.; Huo, J.; Liu, B.; Liu, Z.; Yang, F.; He, K.; Hao, J. Drivers of improved PM2.5 air quality in China from 2013 to 2017. *Proc. Natl. Acad. Sci. U. S. A.* **2019**, *116* (49), 24463−24469.
(9) Li, K.; Jacob, D. J.; Shen, L.; Lu, X.; De Smedt, I.; Liao, H. Increases in surface ozone pollution in China from 2013 to 2019: anthropogenic and meteorological influences. *Atmospheric Chemistry and Physics* **2020**, *20* (19), 11423−11433.
(10) Lu, X.; Zhang, L.; Wang, X.; Gao, M.; Li, K.; Zhang, Y.; Yue, X.; Zhang, Y. Rapid Increases in Warm-Season Surface Ozone and Resulting Health Impact in China Since 2013. *Environmental Science & Technology Letters* **2020**, *7* (4), 240−247.
(11) Li, K.; Jacob, D. J.; Liao, H.; Shen, L.; Zhang, Q.; Bates, K. H. Anthropogenic drivers of 2013−2017 trends in summer surface ozone in China. *Proc. Natl. Acad. Sci. U. S. A.* **2019**, *116* (2), 422−427.
(12) Lu, X.; Zhang, L.; Chen, Y.; Zhou, M.; Zheng, B.; Li, K.; Liu, Y.; Lin, J.; Fu, T.-M.; Zhang, Q. Exploring 2016−2017 surface ozone pollution over China: source contributions and meteorological influences. *Atmospheric Chemistry and Physics* **2019**, *19* (12), 8339−8361.
(13) Liu, Y.; Wang, T. Worsening urban ozone pollution in China from 2013 to 2017 - Part 1: The complex and varying roles of meteorology. *Atmospheric Chemistry and Physics* **2020**, *20* (11), 6305−6321.
(14) Liu, Y.; Wang, T. Worsening urban ozone pollution in China from 2013 to 2017 - Part 2: The effects of emission changes and implications for multi-pollutant control. *Atmospheric Chemistry and Physics* **2020**, *20* (11), 6323−6337.
(15) Dang, R.; Liao, H.; Fu, Y. Quantifying the anthropogenic and meteorological influences on summertime surface ozone in China over 2012−2017. *Science of The Total Environment* **2021**, *754*, 142394.
(16) Yienger, J. J.; Levy, H. Empirical model of global soil-biogenic NOx emissions. *Journal of Geophysical Research* **1995**, *100* (D6), 11447.
(17) Yan, X.; Ohara, T.; Akimoto, H. Statistical modeling of global soil NOxemissions. *Global Biogeochemical Cycles* **2005**, *19* (3), 1.
(18) Su, H.; Cheng, Y. F.; Oswald, R.; Behrendt, T.; Trebs, I.; Meixner, F. X.; Andreae, M. O.; Cheng, P.; Zhang, Y.; Poschl, U. Soil Nitrite as a Source of Atmospheric HONO and OH Radicals. *Science* **2011**, *333* (6049), 1616−1618.
(19) Hudman, R. C.; Moore, N. E.; Mebust, A. K.; Martin, R. V.; Russell, A. R.; Valin, L. C.; Cohen, R. C. Steps towards a mechanistic model of global soil nitric oxide emissions: implementation and space based-constraints. *Atmospheric Chemistry and Physics* **2012**, *12* (16), 7779−7795.
(20) Oswald, R.; Behrendt, T.; Ermel, M.; Wu, D.; Su, H.; Cheng, Y.; Breuninger, C.; Moravek, A.; Mougin, E.; Delon, C.; Loubet, B.; Pommerening-Röser, A.; Sörgel, M.; Pöschl, U.; Hoffmann, T.; Andreae, M. O.; Meixner, F. X.; Trebs, I. HONO Emissions from Soil Bacteria as a Major Source of Atmospheric Reactive Nitrogen. *Science* **2013**, *341* (6151), 1233−1235.
(21) Wang, Y.; Fu, X.; Wang, T.; Ma, J.; Gao, H.; Wang, X.; Pu, W. Large Contribution of Nitrous Acid to Soil-Emitted Reactive Oxidized Nitrogen and Its Effect on Air Quality. *Environ. Sci. Technol.* **2023**, *57* (9), 3516−3526.
(22) Xue, C.; Ye, C.; Zhang, C.; Catoire, V.; Liu, P.; Gu, R.; Zhang, J.; Ma, Z.; Zhao, X.; Zhang, W.; Ren, Y.; Krysztofiak, G.; Tong, S.; Xue, L.; An, J.; Ge, M.; Mellouki, A.; Mu, Y. Evidence for Strong HONO Emission from Fertilized Agricultural Fields and its Remarkable Impact on Regional O3 Pollution in the Summer North China Plain. *ACS Earth and Space Chemistry* **2021**, *5* (2), 340−347.
(23) Wu, D.; Zhang, J.; Wang, M.; An, J.; Wang, R.; Haider, H.; Xu-Ri; Huang, Y.; Zhang, Q.; Zhou, F.; Tian, H.; Zhang, X.; Deng, L.; Pan, Y.; Chen, X.; Yu, Y.; Hu, C.; Wang, R.; Song, Y.; Gao, Z.; Wang, Y.; Hou, L.; Liu, M. Global and Regional Patterns of Soil Nitrous Acid Emissions and Their Acceleration of Rural Photochemical Reactions. *Journal of Geophysical Research: Atmospheres* **2022**, *127* (6), e2021JD036379.
(24) Zhao, Y.; Zhang, L.; Chen, Y.; Liu, X.; Xu, W.; Pan, Y.; Duan, L. Atmospheric nitrogen deposition to China: A model analysis on nitrogen budget and critical load exceedance. *Atmos. Environ.* **2017**, *153*, 32−40.
(25) Liu, L.; Xu, W.; Lu, X.; Zhong, B.; Guo, Y.; Lu, X.; Zhao, Y.; He, W.; Wang, S.; Zhang, X.; Liu, X.; Vitousek, P. Exploring global changes in agricultural ammonia emissions and their contribution to nitrogen deposition since 1980. *Proc. Natl. Acad. Sci. U. S. A.* **2022**, *119* (14), No. e2121998119.
(26) Li, D.; Wang, X.; Sheng, G.; Mo, J.; Fu, J. Soil nitric oxide emissions after nitrogen and phosphorus additions in two subtropical humid forests. *Journal of Geophysical Research* **2008**, *113* (D16), 1.
(27) Lin, J. T. Satellite constraint for emissions of nitrogen oxides from anthropogenic, lightning and soil sources over East China on a high-resolution grid. *Atmospheric Chemistry and Physics* **2012**, *12* (6), 2881−2898.
(28) Huang, Y.; Li, D. Soil nitric oxide emissions from terrestrial ecosystems in China: a synthesis of modeling and measurements. *Sci. Rep.* **2014**, *4* (1), 7406.
(29) Shen, Y.; Xiao, Z.; Wang, Y.; Yao, L.; Xiao, W. Multisource Remote Sensing Based Estimation of Soil NOx Emissions From Fertilized Cropland at High-Resolution: Spatio-Temporal Patterns and Impacts. *Journal of Geophysical Research: Atmospheres* **2022**, *127* (20), e2022JD036741.
(30) Zhang, L.; Wang, T.; Zhang, Q.; Zheng, J.; Xu, Z.; Lv, M. Potential sources of nitrous acid (HONO) and their impacts on ozone: A WRF-Chem study in a polluted subtropical region. *Journal of Geophysical Research: Atmospheres* **2016**, *121* (7), 3645−3662.
(31) Wang, Y.; Fu, X.; Wu, D.; Wang, M.; Lu, K.; Mu, Y.; Liu, Z.; Zhang, Y.; Wang, T. Agricultural Fertilization Aggravates Air Pollution by Stimulating Soil Nitrous Acid Emissions at High Soil Moisture. *Environ. Sci. Technol.* **2021**, *55* (21), 14556−14566.
(32) Liu, P.; Xue, C.; Ye, C.; Liu, C.; Zhang, C.; Wang, J.; Zhang, Y.; Liu, J.; Mu, Y. The Lack of HONO Measurement May Affect the Accurate Diagnosis of Ozone Production Sensitivity. *ACS Environ. Au* **2023**, *3* (1), 18−23.

https://doi.org/10.1021/acs.est.3c01823
Environ. Sci. Technol. XXXX, XXX, XXX−XXX

(33) Wang, R.; Bei, N.; Wu, J.; Li, X.; Liu, S.; Yu, J.; Jiang, Q.; Tie, X.; Li, G. Cropland nitrogen dioxide emissions and effects on the ozone pollution in the North China plain. *Environ. Pollut.* **2022**, *294*, 118617.
(34) Lu, X.; Ye, X.; Zhou, M.; Zhao, Y.; Weng, H.; Kong, H.; Li, K.; Gao, M.; Zheng, B.; Lin, J.; Zhou, F.; Zhang, Q.; Wu, D.; Zhang, L.; Zhang, Y. The underappreciated role of agricultural soil nitrogen oxide emissions in ozone pollution regulation in North China. *Nat. Commun.* **2021**, *12* (1), 5021.
(35) Bey, I.; Jacob, D. J.; Yantosca, R. M.; Logan, J. A.; Field, B. D.; Fiore, A. M.; Li, Q.; Liu, H. Y.; Mickley, L. J.; Schultz, M. G. Global modeling of tropospheric chemistry with assimilated meteorology: Model description and evaluation. *Journal of Geophysical Research: Atmospheres* **2001**, *106* (D19), 23073−23095.
(36) Wang, H.; Lu, X.; Jacob, D. J.; Cooper, O. R.; Chang, K.-L.; Li, K.; Gao, M.; Liu, Y.; Sheng, B.; Wu, K.; Wu, T.; Zhang, J.; Sauvage, B.; Nédélec, P.; Blot, R.; Fan, S. Global tropospheric ozone trends, attributions, and radiative impacts in 1995−2017: an integrated analysis using aircraft (IAGOS) observations, ozonesonde, and multi-decadal chemical model simulations. *Atmospheric Chemistry and Physics* **2022**, *22* (20), 13753−13782.
(37) Gelaro, R.; McCarty, W.; Suarez, M. J.; Todling, R.; Molod, A.; Takacs, L.; Randles, C.; Darmenov, A.; Bosilovich, M. G.; Reichle, R.; Wargan, K.; Coy, L.; Cullather, R.; Draper, C.; Akella, S.; Buchard, V.; Conaty, A.; da Silva, A.; Gu, W.; Kim, G. K.; Koster, R.; Lucchesi, R.; Merkova, D.; Nielsen, J. E.; Partyka, G.; Pawson, S.; Putman, W.; Rienecker, M.; Schubert, S. D.; Sienkiewicz, M.; Zhao, B. The Modern-Era Retrospective Analysis for Research and Applications, Version 2 (MERRA-2). *J. Clim* **2017**, *30* (13), 5419−5454.
(38) Wang, Y.; Jacob, D. J.; Logan, J. A. Global simulation of tropospheric O3-NOx-hydrocarbon chemistry: 1. Model formulation. *Journal of Geophysical Research: Atmospheres* **1998**, *103* (D9), 10713−10725.
(39) Park, R. J. Natural and transboundary pollution influences on sulfate-nitrate-ammonium aerosols in the United States: Implications for policy. *Journal of Geophysical Research* **2004**, *109* (D15), 1.
(40) Parrella, J. P.; Jacob, D. J.; Liang, Q.; Zhang, Y.; Mickley, L. J.; Miller, B.; Evans, M. J.; Yang, X.; Pyle, J. A.; Theys, N.; Van Roozendael, M. Tropospheric bromine chemistry: implications for present and pre-industrial ozone and mercury. *Atmospheric Chemistry and Physics* **2012**, *12* (15), 6723−6740.
(41) Mao, J.; Paulot, F.; Jacob, D. J.; Cohen, R. C.; Crounse, J. D.; Wennberg, P. O.; Keller, C. A.; Hudman, R. C.; Barkley, M. P.; Horowitz, L. W. Ozone and organic nitrates over the eastern United States: Sensitivity to isoprene chemistry. *Journal of Geophysical Research: Atmospheres* **2013**, *118* (19), 11,256−11,268.
(42) Wang, X.; Jacob, D. J.; Downs, W.; Zhai, S.; Zhu, L.; Shah, V.; Holmes, C. D.; Sherwen, T.; Alexander, B.; Evans, M. J.; Eastham, S. D.; Neuman, J. A.; Veres, P. R.; Koenig, T. K.; Volkamer, R.; Huey, L. G.; Bannan, T. J.; Percival, C. J.; Lee, B. H.; Thornton, J. A. Global tropospheric halogen (Cl, Br, I) chemistry and its impact on oxidants. *Atmospheric Chemistry and Physics* **2021**, *21* (18), 13973−13996.
(43) Wesely, M. Parameterization of surface resistances to gaseous dry deposition in regional-scale numerical models. *Atmos. Environ.* **2007**, *41*, 52−63.
(44) Zhang, L. M.; Gong, S. L.; Padro, J.; Barrie, L. A size-segregated particle dry deposition scheme for an atmospheric aerosol module. *Atmos. Environ.* **2001**, *35* (3), 549−560.
(45) Liu, H.; Jacob, D. J.; Bey, I.; Yantosca, R. M. Constraints from 210Pb and 7Be on wet deposition and transport in a global three-dimensional chemical tracer model driven by assimilated meteorological fields. *Journal of Geophysical Research: Atmospheres* **2001**, *106* (D11), 12109−12128.
(46) Amos, H. M.; Jacob, D. J.; Holmes, C. D.; Fisher, J. A.; Wang, Q.; Yantosca, R. M.; Corbitt, E. S.; Galarneau, E.; Rutter, A. P.; Gustin, M. S.; Steffen, A.; Schauer, J. J.; Graydon, J. A.; Louis, V. L. S.; Talbot, R. W.; Edgerton, E. S.; Zhang, Y.; Sunderland, E. M. Gas-particle partitioning of atmospheric Hg(II) and its effect on global mercury deposition. *Atmospheric Chemistry and Physics* **2012**, *12* (1), 591−603.
(47) Lin, J.-T.; McElroy, M. B. Impacts of boundary layer mixing on pollutant vertical profiles in the lower troposphere: Implications to satellite remote sensing. *Atmos. Environ.* **2010**, *44* (14), 1726−1739.
(48) McDuffie, E. E.; Smith, S. J.; O'Rourke, P.; Tibrewal, K.; Venkataraman, C.; Marais, E. A.; Zheng, B.; Crippa, M.; Brauer, M.; Martin, R. V. A global anthropogenic emission inventory of atmospheric pollutants from sector- and fuel-specific sources (1970−2017): an application of the Community Emissions Data System (CEDS). *Earth System Science Data* **2020**, *12* (4), 3413−3442.
(49) Guenther, A. B.; Jiang, X.; Heald, C. L.; Sakulyanontvittaya, T.; Duhl, T.; Emmons, L. K.; Wang, X. The Model of Emissions of Gases and Aerosols from Nature version 2.1 (MEGAN2.1): an extended and updated framework for modeling biogenic emissions. *Geoscientific Model Development* **2012**, *5* (6), 1471−1492.
(50) Murray, L. T.; Jacob, D. J.; Logan, J. A.; Hudman, R. C.; Koshak, W. J. Optimized regional and interannual variability of lightning in a global chemical transport model constrained by LIS/OTD satellite data. *Journal of Geophysical Research: Atmospheres* **2012**, *117* (D20), 1.
(51) Keller, C. A.; Long, M. S.; Yantosca, R. M.; Da Silva, A. M.; Pawson, S.; Jacob, D. J. HEMCO v1.0: a versatile, ESMF-compliant component for calculating emissions in atmospheric models. *Geoscientific Model Development* **2014**, *7* (4), 1409−1417.
(52) Wang, Y.; Ge, C.; Castro Garcia, L.; Jenerette, G. D.; Oikawa, P. Y.; Wang, J. Improved modelling of soil NOx emissions in a high temperature agricultural region: role of background emissions on NO2 trend over the US. *Environmental Research Letters* **2021**, *16* (8), 084061.
(53) Oikawa, P. Y.; Ge, C.; Wang, J.; Eberwein, J. R.; Liang, L. L.; Allsman, L. A.; Grantz, D. A.; Jenerette, G. D. Unusually high soil nitrogen oxide emissions influence air quality in a high-temperature agricultural region. *Nat. Commun.* **2015**, *6* (1), 8753.
(54) Shah, V.; Jacob, D. J.; Li, K.; Silvern, R. F.; Zhai, S.; Liu, M.; Lin, J.; Zhang, Q. Effect of changing NOx lifetime on the seasonality and long-term trends of satellite-observed tropospheric NO2 columns over China. *Atmospheric Chemistry and Physics* **2020**, *20* (3), 1483−1495.
(55) Li, K.; Jacob, D. J.; Liao, H.; Qiu, Y.; Shen, L.; Zhai, S.; Bates, K. H.; Sulprizio, M. P.; Song, S.; Lu, X.; Zhang, Q.; Zheng, B.; Zhang, Y.; Zhang, J.; Lee, H. C.; Kuk, S. K. Ozone pollution in the North China Plain spreading into the late-winter haze season. *Proc. Natl. Acad. Sci. U. S. A.* **2021**, *118* (10), e2015797118.
(56) Wu, D.; Horn, M. A.; Behrendt, T.; Muller, S.; Li, J.; Cole, J. A.; Xie, B.; Ju, X.; Li, G.; Ermel, M.; Oswald, R.; Frohlich-Nowoisky, J.; Hoor, P.; Hu, C.; Liu, M.; Andreae, M. O.; Poschl, U.; Cheng, Y.; Su, H.; Trebs, I.; Weber, B.; Sorgel, M. Soil HONO emissions at high moisture content are driven by microbial nitrate reduction to nitrite: tackling the HONO puzzle. *ISME J.* **2019**, *13* (7), 1688−1699.
(57) Li, Q.; Shi, G.; Shangguan, W.; Nourani, V.; Li, J.; Li, L.; Huang, F.; Zhang, Y.; Wang, C.; Wang, D.; Qiu, J.; Lu, X.; Dai, Y. A 1 km daily soil moisture dataset over China using in situ measurement and machine learning. *Earth System Science Data* **2022**, *14* (12), 5267−5286.
(58) Xue, C.; Ye, C.; Kleffmann, J.; Zhang, W.; He, X.; Liu, P.; Zhang, C.; Zhao, X.; Liu, C.; Ma, Z.; Liu, J.; Wang, J.; Lu, K.; Catoire, V.; Mellouki, A.; Mu, Y. Atmospheric measurements at Mt. Tai - Part II: HONO budget and radical (ROx + NO3) chemistry in the lower boundary layer. *Atmospheric Chemistry and Physics* **2022**, *22* (2), 1035−1057.
(59) Liu, Y.; Lu, K.; Li, X.; Dong, H.; Tan, Z.; Wang, H.; Zou, Q.; Wu, Y.; Zeng, L.; Hu, M.; Min, K. E.; Kecorius, S.; Wiedensohler, A.; Zhang, Y. A Comprehensive Model Test of the HONO Sources Constrained to Field Measurements at Rural North China Plain. *Environ. Sci. Technol.* **2019**, *53* (7), 3517−3525.
(60) He, C.; Lu, X.; Wang, H.; Wang, H.; Li, Y.; He, G.; He, Y.; Wang, Y.; Zhang, Y.; Liu, Y.; Fan, Q.; Fan, S. The unexpected high frequency of nocturnal surface ozone enhancement events over

https://doi.org/10.1021/acs.est.3c01823
Environ. Sci. Technol. XXXX, XXX, XXX−XXX

China: characteristics and mechanisms. *Atmospheric Chemistry and Physics* **2022**, *22* (23), 15243−15261.
(61) Wang, H.; Wang, H.; Lu, X.; Lu, K.; Zhang, L.; Tham, Y. J.; Shi, Z.; Aikin, K.; Fan, S.; Brown, S. S.; Zhang, Y. Increased night-time oxidation over China despite widespread decrease across the globe. *Nature Geoscience* **2023**, *16* (3), 217−223.
(62) Yin, H.; Lu, X.; Sun, Y.; Li, K.; Gao, M.; Zheng, B.; Liu, C. Unprecedented decline in summertime surface ozone over eastern China in 2020 comparably attributable to anthropogenic emission reductions and meteorology. *Environmental Research Letters* **2021**, *16* (12), 124069.
(63) Ye, X.; Wang, X.; Zhang, L. Diagnosing the Model Bias in Simulating Daily Surface Ozone Variability Using a Machine Learning Method: The Effects of Dry Deposition and Cloud Optical Depth. *Environ. Sci. Technol.* **2022**, *56* (23), 16665−16675.
(64) Wang, X.; Fu, T.-M.; Zhang, L.; Cao, H.; Zhang, Q.; Ma, H.; Shen, L.; Evans, M. J.; Ivatt, P. D.; Lu, X.; Chen, Y.; Zhang, L.; Feng, X.; Yang, X.; Zhu, L.; Henze, D. K. Sensitivities of Ozone Air Pollution in the Beijing-Tianjin-Hebei Area to Local and Upwind Precursor Emissions Using Adjoint Modeling. *Environ. Sci. Technol.* **2021**, *55* (9), 5752−5762.
(65) Wang, W.; van der A, R.; Ding, J.; van Weele, M.; Cheng, T. Spatial and temporal changes of the ozone sensitivity in China based on satellite and ground-based observations. *Atmospheric Chemistry and Physics* **2021**, *21* (9), 7253−7269.
(66) Sillman, S. The use of NOy, H2O2, and HNO3as indicators for ozone-NOx-hydrocarbon sensitivity in urban locations. *Journal of Geophysical Research* **1995**, *100* (D7), 14175.
(67) Li, N.; He, Q.; Greenberg, J.; Guenther, A.; Li, J.; Cao, J.; Wang, J.; Liao, H.; Wang, Q.; Zhang, Q. Impacts of biogenic and anthropogenic emissions on summertime ozone formation in the Guanzhong Basin, China. *Atmospheric Chemistry and Physics* **2018**, *18* (10), 7489−7507.
(68) Chen, W.; Guenther, A. B.; Jia, S.; Mao, J.; Yan, F.; Wang, X.; Shao, M. Synergistic effects of biogenic volatile organic compounds and soil nitric oxide emissions on summertime ozone formation in China. *Science of The Total Environment* **2022**, *828*, 154218.
(69) Gao, Y.; Yan, F.; Ma, M.; Ding, A.; Liao, H.; Wang, S.; Wang, X.; Zhao, B.; Cai, W.; Su, H.; Yao, X.; Gao, H. Unveiling the dipole synergic effect of biogenic and anthropogenic emissions on ozone concentrations. *Science of The Total Environment* **2022**, *818*, 151722.
(70) Xue, C. Substantially Growing Interest in the Chemistry of Nitrous Acid (HONO) in China: Current Achievements, Problems, and Future Directions. *Environ. Sci. Technol.* **2022**, *56* (12), 7375−7377.

https://doi.org/10.1021/acs.est.3c01823
Environ. Sci. Technol. XXXX, XXX, XXX−XXX